Drift barriers to quality control when genes are expressed at different levels

Xiong K[*], McEntee JP[†], Porfirio DJ[‡], Masel J[†]

[*]Department of Molecular & Cellular Biology, [†]Department of Ecology & Evolutionary Biology, [‡]Department of Computer Science, University of Arizona, Tucson AZ 85721

7 Corresponding author: Joanna Masel 1041 E Lowell St, Tucson AZ 85721 USA

8 masel@email.arizona.edu Ph. +1 520-626-9888

9 Running title: Drift barriers to quality control

10 Keywords: cryptic genetic variation, stop codon readthrough, robustness, evolvability,

11 transcriptional errors, proofreading

ABSTRACT

Gene expression is imperfect, sometimes leading to toxic products. Solutions take two forms: globally reducing error rates, or ensuring that the consequences of erroneous expression are relatively harmless. The latter is optimal, but because it must evolve independently at so many loci, it is subject to a stringent "drift barrier" – a limit to how weak the effects of a deleterious mutation s can be, while still being effectively purged by selection, expressed in terms of the population size N of an idealized population such that purging requires $s < -1/N$. In previous work, only large populations evolved the optimal local solution, small populations instead evolved globally low error rates, and intermediate populations were bistable, with either solution possible. Here we take into consideration the fact that the effectiveness of purging varies among loci, because of variation in gene expression level and variation in the intrinsic vulnerabilities of different gene products to error. The previously found dichotomy between the two kinds of solution breaks down, replaced by a gradual transition as a function of population size. In the extreme case of a small enough population, selection fails to maintain even the global solution against deleterious mutations, explaining the non-monotonic relationship between effective population size and transcriptional error rate that was recently observed in experiments on *E. coli, C. elegans* and *Buchnera aphidicola*.

INTRODUCTION

In classical population genetic models of idealized populations, the probability of fixation of a new mutant depends sharply on the product of the selection coefficient *s* and the population size *N*. As *s* falls below -1/*N*, fixation probabilities drop exponentially, corresponding to efficient selective purging of deleterious mutations. For $s > -1/N$, random genetic drift makes the fate of new mutants less certain. This nonlinear dependence of fixation probability on *sN* has given rise to the "drift barrier" hypothesis (Lynch 2007), which holds that populations are characterized by a threshold or "barrier" value of the selection coefficient *s*, corresponding to the tipping point at which the removal of deleterious mutations switches between effective and ineffective. In idealized populations described by Wright-Fisher or Moran models, the drift barrier is positioned at $s = \sim -1/N$. Drift barriers also exist, albeit sometimes with less abrupt threshold behavior, in more complex models of evolution in which some assumptions of an idealized population are relaxed (Good and Desai 2014).

The drift barrier theory argues that variation among species in their characteristic threshold values for *s*, thresholds that are equal by definition to the inverse of the selection effective population size N_e, can explain why different species have different characteristics, e.g. streamlined versus bloated genomes (Lynch 2007). The simplest interpretation of the drift barrier would seem to imply that large-N_e species show stricter quality control over all biological processes, e.g. higher fidelity in DNA replication, transcription, and translation, than small-N_e species, because molecular defects in quality control mechanisms are less effectively purged in the latter (Lynch 2010; Traverse and Ochman 2016a).

However, the data reveals more complex patterns. Unsurprisingly, *Buchnera aphidicola*, which has exceptionally low N_e (Mira and Moran 2002; Rispe *et al.* 2004), has a higher transcriptional error rate, at 4.67×10^{-5} (Traverse and Ochman 2016b), than the error rate 4.1×10^{-6} previously reported for *Caenorhabditis elegans* (Gout *et al.* 2013). But to the surprise of the authors, the error rate in large-N_e *Escherichia coli* is highest of all, at 8.23×10^{-5} (Traverse and Ochman 2016b).

A more refined drift barrier theory can explain these findings. As the fitness burden accumulates from the slightly deleterious mutations that a small-N_e species cannot purge, some forms of quality control may evolve as a second line of defense. The ideal solution is to purge all deleterious mutations, even those of tiny effect; when this first line of defense fails, the second line of defense is to ameliorate the cumulative phenotypic consequences of the deleterious mutations that have accumulated (Frank 2007; Rajon and Masel 2011; Warnecke and Hurst 2011; Lynch 2012; Wu and Hurst 2015). In some circumstances, as described further below, strict quality control can act as such an amelioration strategy (Rajon and Masel 2011). The existence of two distinct lines of defense complicates the naive drift barrier logic that large-N_e species should generally exhibit stricter quality control in all molecular processes. The superior performance of large-N_e species in a primary line of defense other than quality control may remove any advantage of strict and costly quality control as a secondary line of defense. This creates a seemingly counter-intuitive pattern in quality control, in which small-N_e species can evolve more faithful processes than large-N_e species such as *E. coli*.

The existence of two substantively different lines of defense was first proposed by Krakauer and Plotkin (2002), who contrasted the "redundancy" of robustness to the consequences of mutational errors with the "antiredundancy" of hypersensitivity to mutations. By positing that redundancy had a cost, they showed that the superior cost-free solution of antiredundancy was available only with large N_e, giving small-N_e species higher levels of "redundancy".

A related argument was made by Rajon and Masel (2011) in the context of mitigating the harms threatened by errors in molecular processes such as translation. Rajon and Masel (2011) distinguished between "local" solutions, where a separate solution is required at each locus, and "global" solutions that can deal with problems at many loci simultaneously. The evolution of extensive quality control mechanisms was deemed a global solution because a single mutation impacting general quality control mechanisms can affect the prevention of gene expression errors at many loci. Note that quality control includes not only mechanisms such as proofreading for preventing errors from happening in the first place, but also mechanisms that reduce downstream damage from errors, e.g. degradation of mRNA molecules that seem faulty. Global quality control should come with a cost in time or energy. The alternative, local solution is to have a benign rather than a strongly deleterious "cryptic genetic sequence" at each locus at which expression errors might occur, making the consequence of an error at that locus relatively harmless. In contrast to the global solution, these local solutions bear no direct fitness cost, but because selection at any one locus is weak, mutations at any one locus pass more easily through the drift barrier, making them more difficult to maintain than global solutions.

95 Both the quality control of Rajon and Masel (2011) and the "redundancy" of Krakauer and
96 Plotkin (2002) to the consequences of mutations are global across loci, and also costly (the
97 former costly by design, the latter costly as a consequence of scaling decisions). Meantime,
98 both the "local" solutions of Rajon and Masel (2011) and the "antiredundancy" of Krakauer and
99 Plotkin (2002) carry no true fitness cost but instead require a large-N_e drift barrier and/or face a
100 "cost of selection" (Haldane 1957) as limits to their adaptation. A mutation disrupting a solution
101 specific to a single locus requires a large value of N_e for its purging, whereas a mutation
102 disrupting a global quality control mechanism will have large fitness consequences and so be
103 easier to purge. The higher-fitness solution is the local one, but it is evolutionarily achievable
104 only with large N_e. With small N_e, we instead expect global solutions such as extensive (and
105 costly) quality control.
106
107 Selection to achieve the local solution by purging deleterious mutations to cryptic sequences
108 (leaving in place genotypes whose cryptic genetic sequences are benign) may be difficult and
109 hence restricted to high-N_e populations. There are, however, reasons to believe that it is not
110 impossible. For example, when the error in question is reading through a stop codon, the local
111 cryptic genetic sequence is the 3'UTR, which is read by the ribosome. One option for a more
112 benign form of this cryptic sequence is the presence of a "backup" stop codon that provides the
113 ribosome with a second and relatively early chance to terminate translation. Such backup stops
114 are common at the first position past the stop in prokaryotes (Nichols 1970). In *Saccharomyces*
115 *cerevisiae*, there is also an abundance of stop codons at the third codon position past the stop
116 (Williams *et al.* 2004). Moreover, conservation at this position depends strongly on whether or

not the codon is a stop, and the overrepresentation of stops at this position is greater in more highly expressed genes (Liang *et al.* 2005). In some ciliates, where the genetic code has been reassigned so that UAA and UAG correspond to glutamine, this overrepresentation is much more pronounced (Adachi and Cavalcanti 2009). As with the consequences of erroneous readthrough, selective pressure on erroneous amino acid misincorporation and/or misfolding (Drummond and Wilke 2008), and on erroneous protein-protein interactions (Brettner and Masel 2012) are also strong enough to shape protein expression and interaction patterns. In the case of transcriptional errors, while both *E. coli* and *B. aphidicola* have high error rates, only *E. coli* shows signs of having evolved a first line of defense in the form of a decreased frequency with which observed transcriptional errors translate into non-synonymous changes, relative to randomly sampled transcriptional errors (Traverse and Ochman 2016a).

Rajon and Masel (2011) found that for intermediate values of N_e that correspond strikingly well to many multicellular species of interest, the evolutionary dynamics of the system were bistable, with either the global or the local solution possible. This is a natural consequence of a positive feedback loop; in the presence of a strict global quality control mechanism, specialized solutions at particular loci are unnecessary and mutations destroying them pass through the drift barrier (we use the expression “pass through the drift barrier” to mean that $0 > s > -1/N$), with their subsequent absence increasing the demand for quality control. Similarly, when specialized solutions predominate, the advantage to quality control is lessened, and resulting higher error rates further increase selection for many locally specialized solutions. If true, this

bistability suggests that historical contingency, rather than current values of N_e, determine which processes are error-prone vs. high-fidelity for populations at intermediate N_e.

In the current work, we note that the model of Rajon and Masel (2011) contained an unrealistic symmetry, namely that the fitness consequence of a molecular error at one locus was exactly equal to that at any other loci. Here we find that with reasonable amounts of variation among loci (e.g. in their expression level or the per-molecule damage from their misfolded form), the bistability disappears. Intermediate solutions evolve instead, where cryptic deleterious sequences are purged only in more highly expressed genes, and quality control evolves to intermediate levels. Variation among loci does not change the previous finding that evolvability tracks the proportion of loci that contain a benign rather than a deleterious cryptic sequence.

The high rate of transcriptional error in *B. aphidicola* can be explained by adding a second bias toward deleterious mutations (in error rate), and hence a second drift barrier to our model. *B. aphidicola* and *E. coli* have high error rates for different reasons; high-fidelity quality control is redundant and unnecessarily expensive in *E. coli*, but unattainable in *B. aphidicola*, leading to similarly high transcriptional error rates.

METHODS

In the following sections, we describe the computational model used to simulate the evolution of different solutions to errors in gene expression. All simulations were run with Matlab (R2014a). Source code for the simulations is available at https://github.com/MaselLab/.

160

161 **Fitness**

162 We follow the additive model of Rajon and Masel (2011), as outlined below, with a few
163 important modifications to accommodate variation in gene expression levels. The model's
164 canonical example is the risk that a ribosome reads through a stop codon during translation.

165

166 The global mitigation strategy is to improve quality control of this gene expression subprocess.
167 We assume that additional quality control that reduces the error rate ρ by some proportion
168 consumes a certain amount of time or comparable resource. Relative to a generation time of 1
169 in the absence of quality control costs, this gives generation time $1 + \delta \ln(1/\rho)$, where δ scales
170 the amount of resources that could have been used in reproduction but are redistributed to
171 quality control. Malthusian fitness is the inverse of generation time, giving

172

173 $$w_{QC} = \frac{1}{1+\delta \ln(1/\rho)} \quad (1)$$

174

175 Following Rajon and Masel (2011), we set $\delta = 10^{-2.5}$, such that reducing ρ from 10^{-2} to 10^{-3}
176 corresponds to a 0.7% reduction in fitness.

177

178 When a readthrough error happens, with frequency ρ, the consequences for fitness depend on
179 the nature of the "cryptic sequence" that lies beyond the stop codon in the 3'UTR. The
180 consequences of mistakes, mutational or otherwise, have a bimodal distribution, being either
181 strongly deleterious (often lethal), or relatively benign, but rarely in between (Eyre-Walker and

Keightley 2007; Fudala and Korona 2009). For example, a strongly deleterious variant of a protein might misfold in a dangerous manner, while a benign variant might fold correctly, although with reduced activity. We assume that alternative alleles of "cryptic genetic sequences" can be categorized according to a benign/deleterious dichotomy.

The local mitigation strategy, the alternative to global quality control, is thus for each cryptic sequence to evolve away from "deleterious" options and toward "benign" options. The local strategy of benign cryptic sequences has no direct fitness cost, but it is nevertheless difficult to evolve at so many loci at once. In contrast, expressing deleterious cryptic sequences has an appreciable cost. This cost scales both with the base rate of expression of the gene, and the proportion ρ of gene products that include the cryptic sequence.

Let the expression of gene i be E_i. We assign the concentration E_i of protein molecules of type i by sampling values of E_i from a $\log_2$-normal distribution with standard deviation σ_E. We define D to be the total frequency of protein expression that would be highly deleterious if expressed in error:

$$D = \frac{\sum_{i \in loci\_with\_del\_crypt\_seq} E_i}{\sum_{i \in loci} E_i} \quad (2)$$

where the numerator sums only over loci that are deleterious and the denominator sums over all loci. This normalization cancels out the effect of the mean value of E_i. We assume the costs of deleterious readthrough are additive across genes, based on the concept that misfolded proteins

(Thomas *et al.* 1995) may aggregate in a non-specific and harmful manner with other proteins and/or membranes (Kourie and Henry 2002), or may simply be expensive to dispose of (Goldberg 2003). After the stop codon is read through, translation will usually end at a backup stop codon within the 3'UTR. Under the assumption of additivity, readthrough events will reduce fitness by $c\rho D$, where c represents the strength of selection against misfolded proteins. Geiler-Samerotte et al. (2011) found that an increase in misfolded proteins of approximately 0.1% of total cellular protein molecules per cell imposed a cost of about 2% to relative growth rate. This gives an estimate of $c = 0.02/0.1\% = 20$.

Readthrough involving benign cryptic sequences does not incur this cost. However, when all cryptic sequences are benign (i.e. $D = 0$), nothing stops ρ from increasing to unreasonably large values, i.e. $\rho > 0.5$, which makes "erroneous" expression into the majority (and hence the "new normal") form. To avoid this scenario, we add a cost in fitness $c\rho^2(1-D)$, whose impact is felt only at high values of ρ. One possible biological interpretation of this second order term is that with probability ρ^2, readthrough occurs not just through the regular stop codon, but also through the backup stop codon at the end of the benign cryptic genetic sequence. To reflect the effects of the double-error scenario under this interpretation, we therefore multiplied the second order term by the probability $\mu_{del}/(\mu_{del}+\mu_{ben})$ that a neutrally evolving cryptic sequence will be deleterious, where μ_{del} is the rate of deleterious-to-benign mutations and μ_{ben} the reverse rate. Other double-error interpretations might involve different constants. In our case, the fitness component representing the cost of misfolded proteins is given by

$$w_{misfolding} = \max(0,1 - c\rho D - c\rho^2(1 - D)\frac{\mu_{del}}{\mu_{del}+\mu_{ben}}) \quad (3)$$

Eq. 3 is a natural extension of the additive model of Rajon and Masel (2011), generalizing to the case of variation in the degree of importance of cryptic loci. Where previous work referred to the number L_{del} of loci having the deleterious rather than benign form, we now distinguish between two measures, L_{del} and D, the latter reporting the proportion of gene product molecules rather than gene loci.

Rajon and Masel (2011) also obtained near-identical results using a very different, multiplicative model. While this suggests that the exact function form of Eq. 3 is unimportant, we chose the additive Eq. 3 model as the more reasonable of the two options. The multiplicative model is premised on loss-of-function of the wild-type proteins, which likely has negligible impact for small losses of a protein whose activity is already close to saturation. In contrast, the additive model is premised on gain-of-negative-function effects of misfolded proteins. These plausibly constitute a major burden on fitness, through a combination of toxicity, disposal costs, and resources spent to replace a faulty molecule with a normal one.

To study evolvability, let a subset of K (typically 50) out of the L (typically 600 or more) loci affect a quantitative trait x, selection on which creates a third fitness component. Error-free expression of locus k, occurring with frequency 1-ρ, has quantitative effect α_k, while expression that involves a benign version of the cryptic sequence has quantitative effect $\alpha_k + \beta_k$. Expression that involves a deleterious version of the cryptic sequence is assumed to result in a

misfolded protein that has no effect on the quantitative trait. We assume that expression level E_k is constant and already factored into values of α_k and β_k. This gives

$$x = \sum_k^K ((1-\rho)\alpha_k + \rho B_k(\alpha_k + \beta_k)) \quad (4)$$

where B_k = 1 indicates a benign cryptic sequence and B = 0 a deleterious one. As in Rajon and Masel (2011), we impose Gaussian selection on x relative to an optimal value x_{opt}

$$w_{trait}(x) = e^{\frac{-(x-x_{opt})^2}{2\sigma_f^2}} \quad (5)$$

where σ_f = 0.5.

Putting the three fitness components together, the relative fitness of a genotype is given by the product

$$w = w_{QC} \times w_{misfolding} \times w_{trait}. \quad (6)$$

Variance in expression levels

We estimated the variance in expression σ_E^2 from PaxDB (Wang *et al.* 2012; Wang *et al.* 2015), which is based on data released by the Global Proteome Machines (GMP) and other sources. We inferred σ_E equal to 2.24 (based on GMP 2012 release) or 3.31 (GMP 2014 release), for *S. cerevisiae*, and 2.93 (GMP 2014 release) for *S. pombe*. Note that while our quantitative

estimate of σ_E comes from variation in the expression levels of different proteins, consideration of variation along other lines might make a standard deviation of 2.25 into a conservative underestimate of the extent of variation. See Fig. S2 for an exploration of this parameter value.

Mutation

There are six kinds of mutation: 1) conversion of a deleterious cryptic sequence to a benign form, 2) conversion from benign to deleterious, 3) change to the error rate ρ, 4) change in the α value of one of the K quantitative trait genes, 5) change in the β value of one of those K genes, and 6) the co-option of a cryptic sequence to become constitutive, replacing the value of replacing α_k with that of $\alpha_k+\beta_k$ and re-initializing B_k and β_k.

It is this sixth kind of mutation that is responsible for the evolvability advantage of the local solution of benign cryptic sequences, providing more mutational raw material by which x might approach x_{opt} (Rajon and Masel 2011; Rajon and Masel 2013). The mutational co-option of a deleterious sequence ($B = 0$) is too strongly deleterious to be favored, even when replacing α_k and β_k might be advantageous. In other words, only benign cryptic sequences are available for mutational co-option. We use the term co-option of a 3'UTR readthrough sequence to refer to the case when a stop codon is lost by mutation, and not just read through by the ribosome (Giacomelli *et al.* 2007; Vakhrusheva *et al.* 2011; Andreatta *et al.* 2015). Mutational co-option for mimicking the consequences of errors other than stop codon readthrough might involve mutations that change expression timing to make a rare protein-protein interaction common, or switch a protein's affinity preference between two alternative partners.

Because we use an origin-fixation approach to simulate evolution (see below), only relative and not absolute mutation rates matter for our outcomes, with the absolute rates setting only the timescale – our rates are therefore effectively unitless. We use the same mutation rates as Rajon and Masel (2011), reduced ten-fold for convenience. Each locus with a benign cryptic sequence mutates to deleterious at rate $\mu_{del} = 2.4\times10^{-8}$, while deleterious loci mutate to benign less often, at rate $\mu_{ben} = 6\times10^{-9}$. Changes to the error rate ρ occur at rate $\mu_{\rho} = 10^{-6}$, while the α and β values of quantitative loci each change with rates $\mu_{\alpha} = 3\times10^{-7}$ and $\mu_{\beta} = 3\times10^{-8}$, respectively. Mutational co-option occurs at each quantitative locus at rate $\mu_{coopt} = 2.56\times10^{-9}$.

Each mutation to ρ increases $\log_{10}\rho$ by an amount sampled from Normal(ρ_{bias}, σ_{ρ}^2). By default, we set $\rho_{bias} = 0$ and $\sigma_{\rho} = 0.2$. To study extremely small populations with drift barriers to evolving even a global solution, we set $\rho_{bias} = 0.256$ and 0.465, corresponding to ratios of ρ-increasing mutations: ρ-decreasing mutations of 9:1 and 99:1, respectively.

A similar scheme for α and β might create, in the global solution case of relaxed selection, a probability distribution of β whose variance increases in an unbounded manner over time (Lande 1975; Lynch and Gabriel 1983). Following previous work (Rajon and Masel 2011; Rajon and Masel 2013), we therefore let mutations alter α and β by an increment drawn from a normal distribution with mean $-\alpha/a$ or $-\beta/a$, with a set to 750, and with standard deviation of σ_m/K in both cases, with σ_m set to 0.5. In the case of neutrality, this mutational process

313 eventually reaches a stationary distribution with mean 0 and standard deviation as calculated in
314 Eq. S3 of Rajon and Masel (2011):
315
316 $$V(a, K, \sigma_m) = \frac{(\sigma_m/K)^2}{1-((a-1)/a)^2} \quad (7)$$
317
318 A co-option at gene *k* changes the gene's quantitative effect to
319
320 $$(1-\rho)(\alpha_k + \beta_k) + \rho B'_k(\alpha_k + \beta_k + \beta'_k) \quad (8)$$
321
322 where B_k' and β_k' are the state and the quantitative effect of a new cryptic sequence created by
323 co-option. Following a co-option mutation at locus *k*, we set the new B_k equal to 1 or 0 with
324 probabilities proportional to μ_{ben} and μ_{del}, and resample the value of β_k from Normal(0, $V(a, K,$
325 $\sigma_m)$).
326
327 **Evolutionary simulations by origin-fixation**
328 We model evolution using an approach known as "weak mutation" (Gillespie 1983), or "origin-
329 fixation" (McCandlish and Stoltzfus 2014). This approximation of population genetics is accurate
330 in the limit where the waiting time until the appearance of the next mutation destined to fix is
331 substantially longer than its subsequent fixation time. The population can then be
332 approximated as genetically homogeneous in any moment in time. While unrealistic for higher
333 mutation rates and larger population sizes, origin-fixation models are computationally
334 convenient. Still more importantly, origin-fixation models, unlike more realistic models with

335 segregating variation, allow the location of the drift barrier to be set externally in the form of
336 the value of the parameter *N*, rather than having the location of the drift barrier emerge from
337 complicated linkage phenomena within the model. Fortunately, for quantitative traits affected
338 by multiple cryptic loci, most evolvability arises from diversity of the effects of co-option of
339 different loci, rather than among the diversity of the effects of co-option from different starting
340 genotypes (Rajon and Masel 2013). This allows us to study evolvability (in the population sense
341 of Wagner (2008)) even in the absence of genetic diversity that is imposed by the origin-fixation
342 formulation.
343
344 Our computationally efficient implementation of origin-fixation dynamics is described in detail
345 in the Supplement, simulating a series of mutations that successfully fix, and the waiting times
346 between each.
347
348 **Initialization and convergence**
349 We initialized the trait optimum at $x_{opt} = 0$. We could have initialized all values of α_k and β_k at
350 zero. However, at steady state, variation in $\sum_1^K \alpha_k$ and $\sum_1^K \beta_k$ is far lower than would be
351 expected from variation in α_k and β_k – this emerges through a process of compensatory
352 evolution (Rajon and Masel 2013). Allowing a realistic steady state to emerge in this way is
353 computationally slow under origin-fixation dynamics, especially when *N* is large. We instead
354 sampled the initial values of α_k and β_k from Normal(0, $V(a, K, \sigma_m)$), where $V(a, K, \sigma_m)$ is defined
355 by Eq. 7, and then subtracted $\bar{\alpha}$ from α_k and $\bar{\beta}$ from β_k, where $\bar{\alpha}$ and $\bar{\beta}$ are the means of a
356 genotype across each of its quantitative loci *k*. This process initializes α_k and β_k to have

variances equal to those of the stationary distributions, while the overall trait value is initialized at the optimal value, zero. This procedure greatly reduces the burn-in computation time needed to achieve a somewhat subtle state of negative within-genotype among-loci correlations. We confirmed that subsequent convergence of the variance of $\sum_1^K \alpha_k$ was fast, occurring in less than 1000 steps, where a "step" is defined to be the fixation of one mutation. We expect $\log_{10}\rho$, D, and variation in $\beta_{k,}$ to converge even faster than variation in α_k.

For the low-ρ initial conditions, ρ was initialized at 10^{-5}, and we initialized the benign vs. deleterious status of cryptic sequences at the neutral mutational equilibrium, choosing exactly $L\times\mu_{del}/(\mu_{del}+\mu_{ben})$ (rounded to the nearest integer) to be deleterious, independently of their different values of E. For the high-ρ initial conditions, we set ρ to 10^{-1}, and made all cryptic sequences benign.

We ran simulations for 10^5 steps, recording information at fixed times (measured in terms of waiting times), corresponding to approximately every 1000 steps on average, and hence yielding about 100 timepoints. To summarize the evolutionary outcome, we calculated the arithmetic means of $\log_{10}\rho$, of L_{del}, and of D among the last 20 timepoints, i.e. approximating steps 0.8×10^5-1×10^5.

Evolvability

After adaptation to a trait optimum of $x_{opt} = 0$ had run to convergence (i.e. after 10^5 steps), we changed x_{opt} to 2, forcing the quantitative trait to evolve rapidly. This allows the co-option of

benign cryptic sequences an opportunity to increase evolvability. We measured evolvability in two ways: as the inverse of the waiting time before trait *x* exceeded 1, and the inverse of the waiting time before the population recovered half of the fitness it lost after x_{opt} changed. By default, we present results showing evolvability as time to fitness recovery; evolvability as time to trait recovery is shown only in Fig. S3.

We want our measures of evolvability to reflect a genotype's potential to generate beneficial mutations, but this goal was complicated by population size. A large population finds a given beneficial mutation faster than a small population does, inflating the total fixation flux $\sum_{i \in beneficial\_mutation} \mu_i N P_{fix}(i)$, where $\mu_i N$ is the influx of mutations of beneficial type *i* and P_{fix} is their probability of fixation (the latter described by Eq. 9 in the supplemental material), in direct proportion to population size. We therefore divided our evolvability measures by the population size to correct for this effect. This normalization converts the population-level evolvability measure into a measure of the population-size-independent evolvability of a single individual that has the genotype of interest.

RESULTS

Recall that in the absence of variation in expression among genes, there are two solutions to handle erroneous expression due to stop codon readthrough: at high population size *N*, the local solution purges all deleterious cryptic sequences, making high rates of readthrough harmless, while at low *N*, the global solution reduces the rate of readthrough, allowing deleterious cryptic sequences to accumulate near-neutrally. At intermediate *N*, we see

401 bistability, with either solution possible, depending on starting conditions (Fig. 1, $\sigma_E = 0$). It is
402 important to note that we use the word "bistability" loosely. Strictly speaking, bistability means
403 that the system has two stable steady states (here a state is defined by readthrough rate and
404 the exact property of each cryptic sequence), i.e. two attractors. But in a stochastic model,
405 there are no attractors in the strict sense of the word, only a stationary distribution of states.
406 We use the term bistability to refer to the case where the stationary distributions of states has
407 two modes. Transitions between the two modes are rare, therefore the two modes can be
408 loosely interpreted as the two attractors of the system.
409
410 Our results qualitatively reproduce the bistability reported by Rajon and Masel (2011) for the
411 case where there is no expression variation among genes, though the range of values of *N*
412 leading to bistability is smaller than that found in Rajon and Masel (2011) in which a full Wright-
413 Fisher simulation is used. The smaller range of bistability in our model could be caused by the
414 ease with which long-term evolution is captured using an origin-fixation framework, or by other
415 subtle differences between the approaches, e.g. the greater ease of compensatory evolution
416 under Wright-Fisher dynamics than under origin-fixation. We chose origin-fixation mainly to
417 reduce the computational burden, which for our study was increased by the need to track
418 individual loci, in contrast to previous work that needed only to track the number of loci with
419 deleterious cryptic sequence, without distinguishing their identities (Rajon and Masel 2011;
420 Rajon and Masel 2013).
421

422 However, bistability vanishes with variation in expression among genes (Fig. 1, σ_E = 2.25 and σ_E
423 = 3.5). To understand why, consider a population initialized at low readthrough rate (ρ) and many
424 deleterious cryptic sequences. Because the strength of selection against a deleterious cryptic
425 sequence at locus *i* is proportional to ρE_i (the effect of a locus *i* on *D* in Eq. 3 is proportional to
426 E_i), purging works at the most highly expressed loci, even when ρ is low. This lowers the
427 proportion *D* of readthrough events that are deleterious, which relaxes selection for high fidelity,
428 leading to an increase in ρ. As ρ increases, loci with lower E_i become subject to effective purging,
429 which further reduces *D*, which feeds back to increase ρ further. Because E_i is log-normally
430 distributed, but contributes linearly to selection via *D*, each round of the feedback loop involves
431 smaller changes than the last. Eventually, the changes are too small for selection on them to
432 overcome mutation bias in favor of deleterious sequences. Similarly, when a population is
433 initialized at high ρ, mutational degradation begins at low E_i sites and arrests when selection is
434 strong enough to kick in. The point of balance between mutation bias and selection defines a
435 single intermediate attractor for $\sigma_E \geq 2.25$, instead of the bistable pair of attractors found for
436 uniform E_i ($\sigma_E = 0$). For $\sigma_E < 2.25$, bistability is still found, but for a narrower range of population
437 sizes than in the absence of variation (Fig. S2).
438
439 Even though bistability is not found for σ_E = 2.25, there is still a fairly sharp dichotomy, with
440 solutions being either local (high ρ and low L_{del}) or global (low ρ and high L_{del}), and intermediate
441 solutions found only for a very restrictive range of *N*, following a sigmoidal curve (Fig. 1**a** and 1**c**).
442 Increasing variation in expression among genes blurs the boundary between the local solution
443 and the global solution. Intermediate solutions are found for broader ranges of *N* as expression

444 variance σ_E increases to 3.5. The trend, as expression variance σ_E increases from 0, is to first
445 replace bistability with a limited range of intermediate solutions (σ_E = 2.25), and then for the
446 intermediate solutions to become more prevalent, with extreme local and global solutions
447 becoming less attainable as σ_E > 2.25.
448
449 The breakdown of the local solution begins with intermediate values of L_{del}, while the breakdown
450 of the global solution begins with intermediate values of ρ and D (Fig. 1 **a**-**c**). The breakdown of
451 global solutions involves high-expression loci (Fig. 2), which affect D more than L_{del}. In contrast,
452 the breakdown of local solutions involves low-expression loci (Fig. 2), which affect L_{del} more than
453 D. Because ρ is better described as co-evolving with D than with L_{del}, as explained earlier,
454 intermediate values of ρ are seen more in the breakdown of global than local solutions.
455
456 A primary motivation behind characterizing the two solutions is that the local solution was found
457 to have dramatically higher evolvability than the global solution (Rajon and Masel 2011). We
458 therefore check whether this conclusion still broadly stands in the presence of variance in
459 expression levels. The local solution promotes evolvability by making benign cryptic sequences
460 available for co-option. Differences in evolvability between genotypes should therefore be
461 largely determined by the fraction of quantitative trait loci that carry benign rather than
462 deleterious cryptic sequences. In agreement with this, evolvability inversely mirrors L_{del}, as a
463 function of population size, i.e., evolvability (Fig. 1**d**) resembles L_{del} (Fig. 1**c**) far more than it
464 resembles ρ (Fig. 1**a**) or D (Fig. 1**b**).
465

466 The distinction between global and location solutions becomes more extreme when the mutation
467 bias toward deleterious rather than benign cryptic sequences is increased from 4:1 ratio to a 99:1
468 ratio, but persists even when the mutation bias is eliminated in favor of a 1:1 ratio (Fig. 3). In the
469 absence of mutation bias, there is less evolvability to be gained by the local relative to the global
470 solution, since half the quantitative loci are available for co-option regardless (Fig. 3**c**).
471 Nevertheless, a small evolvability advantage to the local solution can still be observed (Fig. 3**d**).
472 In any case, assuming mutation bias toward deleterious options is biologically reasonable, and
473 Fig. 3 shows that results are not sensitive to the quantitative strength of our assumption on this
474 count.
475
476 When we also account for mutation bias that tends to increase rather than decrease the error
477 rate ρ, our model can explain the previously puzzling observation that the rate of
478 transcriptional errors in small-N_e endosymbiont bacteria *Buchnera* is so much higher than that
479 of *C. elegans*, and almost as high as that of large-N_e *E. coli* (McCandlish and Plotkin 2016;
480 Traverse and Ochman 2016b). In extremely small populations, even the global solution is
481 subject to a drift barrier, making ρ higher than its optimal value. For N so small such that most
482 ρ-increasing mutations pass through the drift barrier, ρ can be almost as large as that in large
483 populations (Fig. 4**a**). Despite their high error rates, these extremely small populations also
484 carry heavy loads of deleterious cryptic products (Fig. 4**b** and **c**), consistent with the fact that in
485 *B. aphidicola*, unlike *E. coli*, selection is unable to reduce the fraction of non-synonymous
486 transcriptional errors that are non-synonymous (Traverse and Ochman 2016a). High ρ shows
487 the absence of a global solution, while high D and L_{del} show the absence of a local solution;

488 neither solution is found for a sufficiently small population. Similar error rates in large and small
489 populations can also be found, given bias in mutations to ρ, when there is no variation in
490 expression levels (Fig. S5).
491
492 The parameters in our model can be classified into three groups, and the exploration of their
493 values is summarized in Table S1. The first group controls selection coefficients relevant to the
494 global vs. local solution outcome: the variance in expression levels (σ_E^2), the number of loci (L,
495 Fig. S4), the cost of misfolded protein molecules (c), and the cost of quality control (δ, Fig. S6).
496 The second group controls mutation bias relevant to the global vs. local solution outcome: the
497 frequency with which mutations turn deleterious cryptic sequences benign versus the reverse
498 (μ_{ben}:μ_{del}), whether mutations to ρ tend to increase or decrease it ($P_{+\rho}$:$P_{-\rho}$), and variance in the
499 magnitude of mutations to ρ (σ_ρ^2, Fig. S7). The third group contains all the parameters that
500 control the evolution of quantitative traits encoded by a minority of loci relevant to the
501 evolvability properties. Because our focus in this manuscript is on the evolution of global vs.
502 local solutions, not on the precise details of the relationship between local solutions and
503 evolvability, these parameter values were explored less.
504
505 The influence of σ_E^2 dominates our results. Its effect in eliminating bistability holds, with the
506 one exception that very "cheap" quality control could partially restore bistability (Fig. S6).
507 Otherwise, we found that three parameters – c, δ, and μ_{ben}:μ_{del} – are the main determinants of
508 the population size at which the transition between global and local solutions takes place, and
509 of the exact error rate that evolves for global and local solutions (Table S1). The other

parameters in the first and second groups have little or no influence on the evolutionary outcomes that we study. In general, parameters in the first group, controlling selection, have stronger effects than the second group, controlling mutation bias.

DISCUSSION

When genes vary in their expression levels, the dichotomy between the local and global solutions is replaced by a continuous transition. Very large populations still resemble the local solution, although mutations making cryptic sequences deleterious still pass through the drift barrier in the occasional low-expression gene. Very small populations still resemble the global solution, although mutations making cryptic sequences deleterious may still be effectively purged in a few high-expression genes; because their high expression disproportionately affects the burden from misexpression, this relaxes expression for high fidelity, leading to less strict quality control.

In agreement with drift barrier theory, large-N_e *E. coli* exhibits a local solution – a tendency for transcription errors to have synonymous effects – while small-N_e *B. aphidicola* does not (Traverse and Ochman 2016a). While as predicted, the global solution of low transcriptional error rates does not obey the naïve drift barrier expectation of being higher in *B. aphidicola* than in *E. coli* (Traverse and Ochman 2016a), nor are transcription error rates drastically lower in *B. aphidicola* as predicted by previous theory on the interplay between global and local solutions (Rajon and Masel 2011; McCandlish and Plotkin 2016). This significantly lower rate relative to *E. coli* is, however, found in intermediate-N_e *C. elegans*. Where previous work (Rajon

and Masel 2011) explained only the relative rates for *E. coli* and *C. elegans*, here we also explain the high error rate of *B. aphidicola* by taking into account a drift barrier on the global solution of low error rates. This drift barrier is significant because of mutation bias towards higher error rates. Small *B. aphidicola* populations have higher error rates than *C. elegans* because it is the best that evolution at low N_e can manage, despite the deleterious consequences; large *E. coli* populations have similarly high error rates because with the worst consequences of error already purged, they don't need to incur the cost that quality control entails.

With small amounts of variation in expression among genes, the range of intermediate values of N_e for which bistability is found shrinks. With more variation, bistability vanishes in favor of a sigmoidal transition between global and local solutions. With still more, the sigmoid is smoothed out, and intermediate solutions are found for most values of N_e.

To interpret our results correctly, we must therefore estimate the degree to which genes vary. The results presented here focus on two estimates of the variation in log-expression in yeast, namely standard deviations of 2.25 and 3.5. However, variation among genes in the deleterious consequences of misfolding, in addition to variation in expression levels, might make larger standard deviations a better model of reality, further supporting a continuum of intermediate solutions. In other words, the value of c in Eq. 3 may vary among genes. Note that apart from the second-order ρ^2 term, the cost of a deleterious misfolded protein i depends only on the product of c_i and expression level E_i. Given log-normal distributions of c_i and expression level E_i, the variance of the log-product is equal to the sum of the two log-variances, so we can

554 transform this scenario into one where c is constant, and σ_E^2 is equal to this sum. This can be
555 done because changing c_i and E_i only affects $w_{misfolding}$ and not other factors such as the
556 magnitude of a locus's influence on the quantitative trait. In other words, adding variation to c
557 is almost equivalent to increasing the variance in expression levels.
558
559 The values of μ_{del} and μ_{ben} may also vary among genes. Drift barrier effects operate via the
560 effect of population size on the fate of deleterious not beneficial mutations – if purging is
561 efficient, then the beneficial mutation rate does not matter, because a single beneficial
562 mutation is enough. We therefore focus on μ_{del}. The inclusion of a benign-to-deleterious
563 mutation M_i at locus i depends on the product of μ_{del} at locus i and M_i's probability of fixation.
564 It seems likely that variation among genes in the probability that a deleterious cryptic sequence
565 becomes fixed will swamp variation in the deleterious mutation rate – variation in expression
566 levels cause the former to vary over orders of magnitude. Note that as for the case of variation
567 in c, it is possible to construct a manipulation of E_i that has the same effect on the relevant
568 product, via the probability of fixation, as would occur given a change in μ_{del}. While this case is
569 less neat than for the product c_iE_i, it illustrates that a model of variation in expression levels
570 can reflect, to some extent, the effect of variation in μ_{del}.
571
572 Our model makes three critical assumptions, which must be understood for the results to be
573 interpreted appropriately. First, a "locus" in our model consists of one regular and one cryptic
574 sequence. The primary example that we used to parameterize the simulations posits an entire
575 protein-coding gene as the regular sequence, and the extended polypeptide resulting from stop

576 codon readthrough as the cryptic alternative. In the example of transcriptional errors, a locus is
577 a single codon, with its corresponding amino acid being the regular sequence, and the most
578 common consequence of a transcriptional error as the cryptic. The case of one regular
579 sequence and many alternative cryptic ones has not been modeled. Similarly, proteins may
580 each have a regular fold or binding partner, and our model considers the contrast between this
581 state and a single cryptic alternative.
582
583 Second, we assume that the rate of gene expression errors is set globally, across all loci. In
584 reality, individual context may also affect the error rate, giving error rates a local solution
585 aspect as well. A model of three rather than two interacting solutions – global error rates, local
586 error rates, and local robustness to the consequences of error – remains for future work.
587 Perhaps highly expressed genes will have both more benign cryptic sequences and lower rates
588 of error, or perhaps the evolution of one kind of local solution will alleviate the need for
589 another. Testing this empirically requires data on site-specific error rates and on a credible
590 marker for the benign status of members of an identifiable class of cryptic sequences. Such
591 tools are now becoming available, and indeed we recently found a positive correlation between
592 a large number of readthrough errors at a particular stop codon and the benign status of the
593 readthrough translation product (Kosinski et al., manuscript in preparation). We also reanalyzed
594 the data of Traverse and Ochman (2016a) to find that highly expressed transcripts have lower
595 transcriptional error rates (unpublished result).
596

Finally, we assume that the consequences of errors have a bimodal distribution: either highly deleterious or largely benign, but rarely in between. In other words, we assume that a basic phenomenon in biology is that changes tend to either break something, or to tinker with it. There are a variety of lines of evidence supporting this intuitively reasonable assumption (Fudala and Korona 2009; Wylie and Shakhnovich 2011).

ACKNOWLEDGEMENTS

This work was supported by the John Templeton Foundation [grant number 39667]. DJP was also funded by the Undergraduate Biology Research Program at the University of Arizona. We thank Lilach Hadany, Yoav Ram, and other members of the Hadany group for helpful discussions that prompted us to explore variation in expression. We thank Paul Nelson for developing the idea of local error rates as an expansion of our model, Ben Wilson for help with R, and Etienne Rajon, Yoav Ram, Tobias Warnecke, and one anonymous reviewer for helpful comments on the manuscript. We also thank Charles Traverse and Howard Ochman for sharing their data on transcriptional errors. An allocation of computer time from the UA Research Computing High Performance Computing (HPC) and High Throughput Computing (HTC) at the University of Arizona is gratefully acknowledged.

LITERATURE CITED

Adachi, M., and A. R. O. Cavalcanti, 2009 Tandem Stop Codons in Ciliates That Reassign Stop Codons. J. Mol. Evol. 68**:** 424-431.

617 Andreatta, M. E., J. A. Levine, S. G. Foy, L. D. Guzman, L. J. Kosinski *et al.*, 2015 The Recent De
618 Novo Origin of Protein C-Termini. Genome Biology and Evolution 7**:** 1686-1701.
619 Brettner, L. M., and J. Masel, 2012 Protein stickiness, rather than number of functional protein-
620 protein interactions, predicts expression noise and plasticity in yeast. BMC Systems
621 Biology 6**:** 128.
622 Drummond, D. A., and C. O. Wilke, 2008 Mistranslation-Induced Protein Misfolding as a
623 Dominant Constraint on Coding-Sequence Evolution. Cell 134**:** 341-352.
624 Eyre-Walker, A., and P. D. Keightley, 2007 The distribution of fitness effects of new mutations.
625 Nat. Rev. Genet. 8**:** 610-618.
626 Frank, S. A., 2007 Maladaptation and the Paradox of Robustness in Evolution. PLoS ONE 2**:**
627 e1021.
628 Fudala, A., and R. Korona, 2009 Low frequency of mutations with strongly deleterious but
629 nonlethal fitness effects. Evolution 63**:** 2164-2171.
630 Geiler-Samerotte, K. A., M. F. Dion, B. A. Budnik, S. M. Wang, D. L. Hartl *et al.*, 2011 Misfolded
631 proteins impose a dosage-dependent fitness cost and trigger a cytosolic unfolded
632 protein response in yeast. Proc. Natl. Acad. Sci. U.S.A. 108**:** 680-685.
633 Giacomelli, M. G., A. S. Hancock and J. Masel, 2007 The conversion of 3' UTRs into coding
634 regions. Mol. Biol. Evol. 24**:** 457-464.
635 Gillespie, J. H., 1983 Some properties of finite populations experiencing strong selection and
636 weak mutation. Am. Nat. 121**:** 691-708.
637 Goldberg, A. L., 2003 Protein degradation and protection against misfolded or damaged
638 proteins. Nature 426**:** 895-899.

639 Good, B. H., and M. M. Desai, 2014 Deleterious Passengers in Adapting Populations. Genetics
640 198: 1183-1208.
641 Gout, J.-F., W. K. Thomas, Z. Smith, K. Okamoto and M. Lynch, 2013 Large-scale detection of in
642 vivo transcription errors. Proc. Natl. Acad. Sci. U.S.A. 110: 18584-18589.
643 Haldane, J. B. S., 1957 The cost of natural selection. J. Genetic. 55: 511-524.
644 Kourie, J. I., and C. L. Henry, 2002 Ion channel formation and membrane-linked pathologies of
645 misfolded hydrophobic proteins: The role of dangerous unchaperoned molecules. Clin.
646 Exp. Pharmacol. Physiol. 29: 741-753.
647 Krakauer, D. C., and J. B. Plotkin, 2002 Redundancy, antiredundancy, and the robustness of
648 genomes. Proc. Natl. Acad. Sci. U.S.A. 99: 1405-1409.
649 Lande, R., 1975 The maintenance of genetic variability by mutation in a polygenic character
650 with linked loci. Genet. Res. 26: 221-235.
651 Liang, H., A. R. O. Cavalcanti and L. F. Landweber, 2005 Conservation of tandem stop codons in
652 yeasts. Genome Biol. 6: R31.
653 Lynch, M., 2007 *The origins of genome architecture*. Sinauer Associates, Sunderland.
654 Lynch, M., 2010 Evolution of the mutation rate. Trends Genet. 26: 345-352.
655 Lynch, M., 2012 Evolutionary layering and the limits to cellular perfection. Proc. Natl. Acad. Sci.
656 U.S.A. 109: 18851-18856.
657 Lynch, M., and W. Gabriel, 1983 Phenotypic evolution and parthenogenesis. Am. Nat. 122: 745-
658 764.
659 McCandlish, D. M., and J. B. Plotkin, 2016 Transcriptional errors and the drift barrier. Proc. Natl.
660 Acad. Sci. U.S.A. 113 136-3138

McCandlish, D. M., and A. Stoltzfus, 2014 Modeling Evolution Using the Probability of Fixation: History and Implications. Q. Rev. Biol. 89: 225-252.

Mira, A., and N. A. Moran, 2002 Estimating Population Size and Transmission Bottlenecks in Maternally Transmitted Endosymbiotic Bacteria. Microbial Ecology 44: 137-143.

Nichols, J. L., 1970 Nucleotide Sequence from the Polypeptide Chain Termination Region of the Coat Protein Cistron in Bacteriophage R17 RNA. Nature 225: 147-151.

Rajon, E., and J. Masel, 2011 The evolution of molecular error rates and the consequences for evolvability. Proc. Natl. Acad. Sci. U.S.A. 108: 1082-1087.

Rajon, E., and J. Masel, 2013 Compensatory Evolution and the Origins of Innovations. Genetics 193: 1209-1220.

Rispe, C., F. Delmotte, R. C. H. J. van Ham and A. Moya, 2004 Mutational and Selective Pressures on Codon and Amino Acid Usage in Buchnera, Endosymbiotic Bacteria of Aphids. Genome Res. 14: 44-53.

Thomas, P. J., B.-H. Qu and P. L. Pedersen, 1995 Defective protein folding as a basis of human disease. Trends Biochem. Sci. 20: 456-459.

Traverse, C. C., and H. Ochman, 2016a Conserved rates and patterns of transcription errors across bacterial growth states and lifestyles. Proc. Natl. Acad. Sci. U.S.A. 113: 3311-3316

Traverse, C. C., and H. Ochman, 2016b Correction for Traverse and Ochman, Conserved rates and patterns of transcription errors across bacterial growth states and lifestyles. Proc. Natl. Acad. Sci. U.S.A. 113: E4257-E4258.

Vakhrusheva, A., M. Kazanov, A. Mironov and G. Bazykin, 2011 Evolution of Prokaryotic Genes by Shift of Stop Codons. J. Mol. Evol. 72: 138-146.

683 Wagner, A., 2008 Robustness and evolvability: a paradox resolved. Proc. R. Soc. Lond. Ser. B-
684 Biol. Sci. 275**:** 91-100.
685 Wang, M., C. J. Herrmann, M. Simonovic, D. Szklarczyk and C. von Mering, 2015 Version 4.0 of
686 PaxDb: Protein abundance data, integrated across model organisms, tissues, and cell-
687 lines. Proteomics 15**:** 3163-3168.
688 Wang, M., M. Weiss, M. Simonovic, G. Haertinger, S. P. Schrimpf *et al.*, 2012 PaxDb, a Database
689 of Protein Abundance Averages Across All Three Domains of Life. Mol. Cell. Proteomics
690 11**:** 492-500.
691 Warnecke, T., and L. D. Hurst, 2011 Error prevention and mitigation as forces in the evolution of
692 genes and genomes. Nat Rev Genet 12**:** 875-881.
693 Williams, I., J. Richardson, A. Starkey and I. Stansfield, 2004 Genome-wide prediction of stop
694 codon readthrough during translation in the yeast *Saccharomyces cerevisiae*. Nucleic
695 Acids Res. 32**:** 6605-6616.
696 Wu, X., and L. D. Hurst, 2015 Why Selection Might Be Stronger When Populations Are Small:
697 Intron Size and Density Predict within and between-Species Usage of Exonic Splice
698 Associated cis-Motifs. Mol. Biol. Evol. 32**:** 1847-1861.
699 Wylie, C. S., and E. I. Shakhnovich, 2011 A biophysical protein folding model accounts for most
700 mutational fitness effects in viruses. Proc. Natl. Acad. Sci. U.S.A. 108**:** 9916-9921.

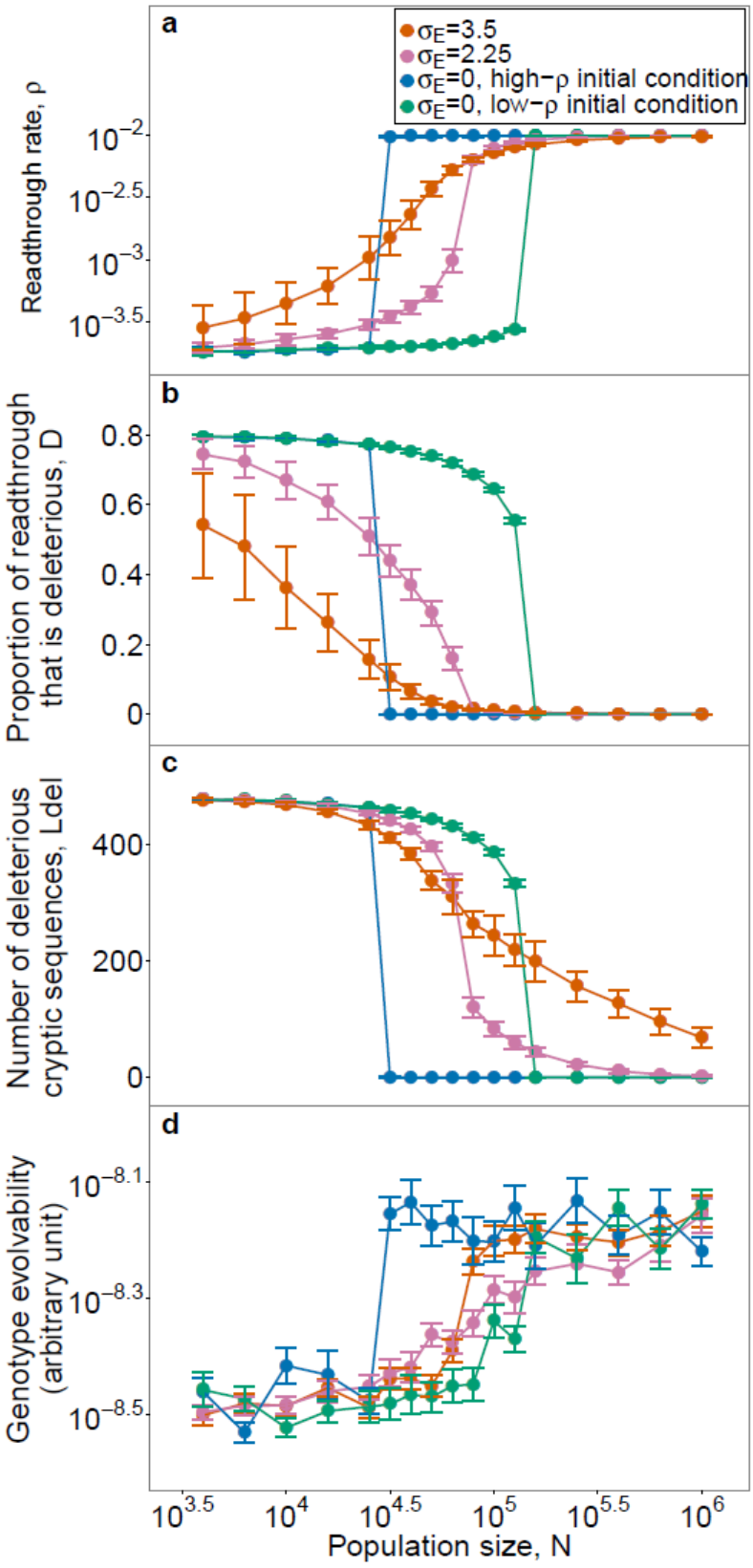

Figure 1: Evolutionary dynamics are bistable in the absence of variation in gene expression ($\sigma_E = 0$), but not with variation in gene expression ($\sigma_E = 2.25$ and $\sigma_E = 3.5$). We calculated the average values of ρ, D, and L_{del} towards the end of the simulations, and then measured the genotype evolvability after changing the optimal trait value (see Methods for details). For each value of N, 20 simulations were initialized at high-ρ conditions and 15 at low-ρ conditions. For $\sigma_E = 2.25$ and $\sigma_E = 3.5$, simulations from the two initial conditions reached indistinguishable endpoints (Fig. S1), so the results were pooled. The increment in N is $10^{0.1}$ between $10^{4.4}$ and $10^{5.2}$ to increase resolution, and is $10^{0.2}$ elsewhere. At $\sigma_E = 0$, D is indistinguishable from zero for $N \geq 10^{5.2}$ under high-ρ conditions and for $N \geq 10^{4.7}$ under low-ρ conditions, corresponding to L_{del} being effectively zero. In contrast, when $\sigma_E = 2.25$ or 3.5, because the weakness of selection on low-expression genes prevents L_{del} from falling all the way to zero, D never quite reaches zero either, despite appearing superimposable in **b**. For **a** to **c**, data is shown as mean$\pm$SD. For evolvability (**d**), data is shown as mean$\pm$SE. For **a** and **d**, these apply to log-transformed values. Evolvability is based on time to fitness recovery; see Fig. S3 for similar results based on time to trait recovery. $L = 600$.

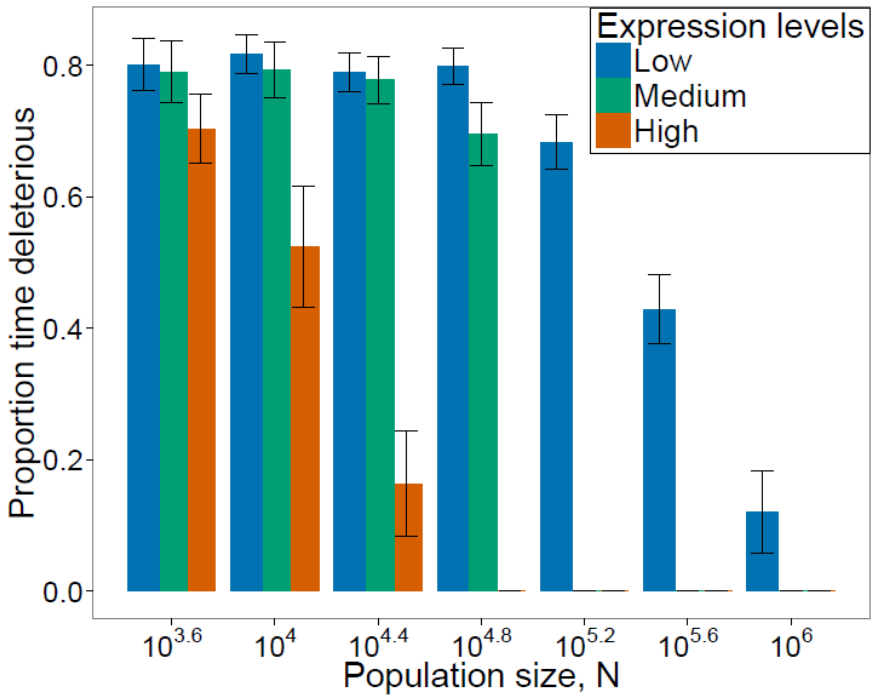

Figure 2: The effectiveness of purging a cryptic sequence of deleterious mutations depends on its expression level. We examined the states of the cryptic sequences of the loci with the 10 highest, the 10 lowest, and the 10 median expression levels among the 600 loci in each of the simulations showed in Fig. 1 (σ_E = 2.25). We counted how often each locus contained a deleterious cryptic sequence among the last 20 timepoints we had collected from that simulation. Bars represent the proportion of time that each of the 10 loci carried a deleterious cryptic sequence, averaged over 20 replicates, and shown as mean $\pm$SD . Simulations were initialized at low-ρ conditions.

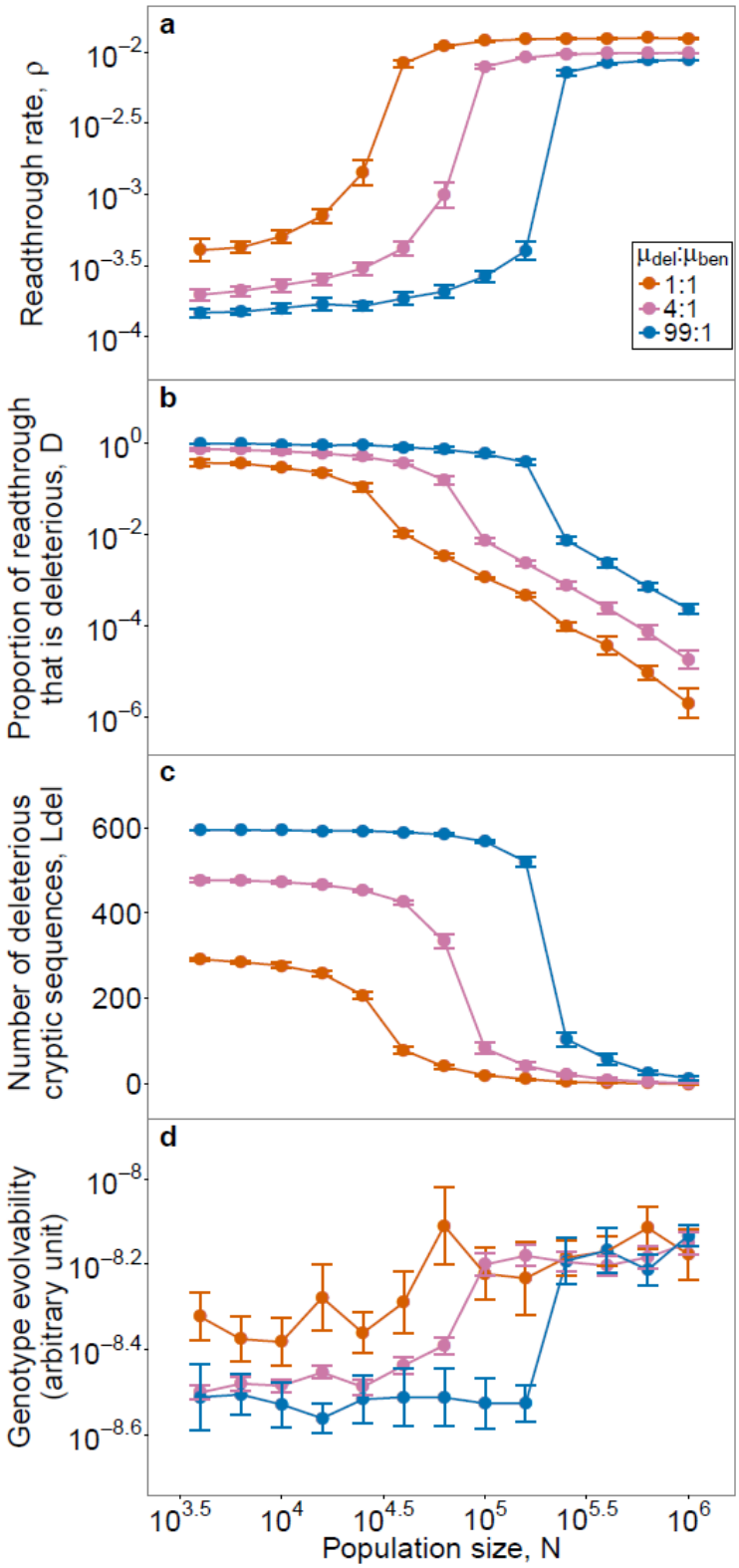

Figure 3: Results become more extreme when the mutation bias in the state of a cryptic sequence is increased from 4:1 ratio to a 99:1 ratio, but do not disappear completely when the mutation bias is eliminated in favor of a 1:1 ratio. The location of the drift barrier shifts as a function of mutation bias, but the dichotomy between local and global solutions (as seen in values of ρ and D) is not sensitive to relaxing the mutation bias. The advantage of the local solution with respect to evolvability (as seen in **d** and mirrored in L_{del} (**c**)) is more sensitive to lack of mutation bias, but is still visible even with a 1:1 ratio. To compare results across different mutation biases, we kept the sum of the two mutation rates constant. For the low-ρ initial conditions, the number of deleterious cryptic sequences was initialized at the neutral mutational equilibrium of $L \times \mu_{del}/(\mu_{del}+\mu_{ben})$ (rounded to the nearest integer). For $\mu_{del}:\mu_{ben}$ = 4:1, we reused the results shown in Fig. 1. For the other ratios, five replicates were run for each initial condition, and pooled. For panels **a** to **c**, data is shown as mean±SD. For panel **d**, data is shown as mean±SE. For **a** and **d**, these apply to log-transformed values. L = 600 and σ_E = 2.25.

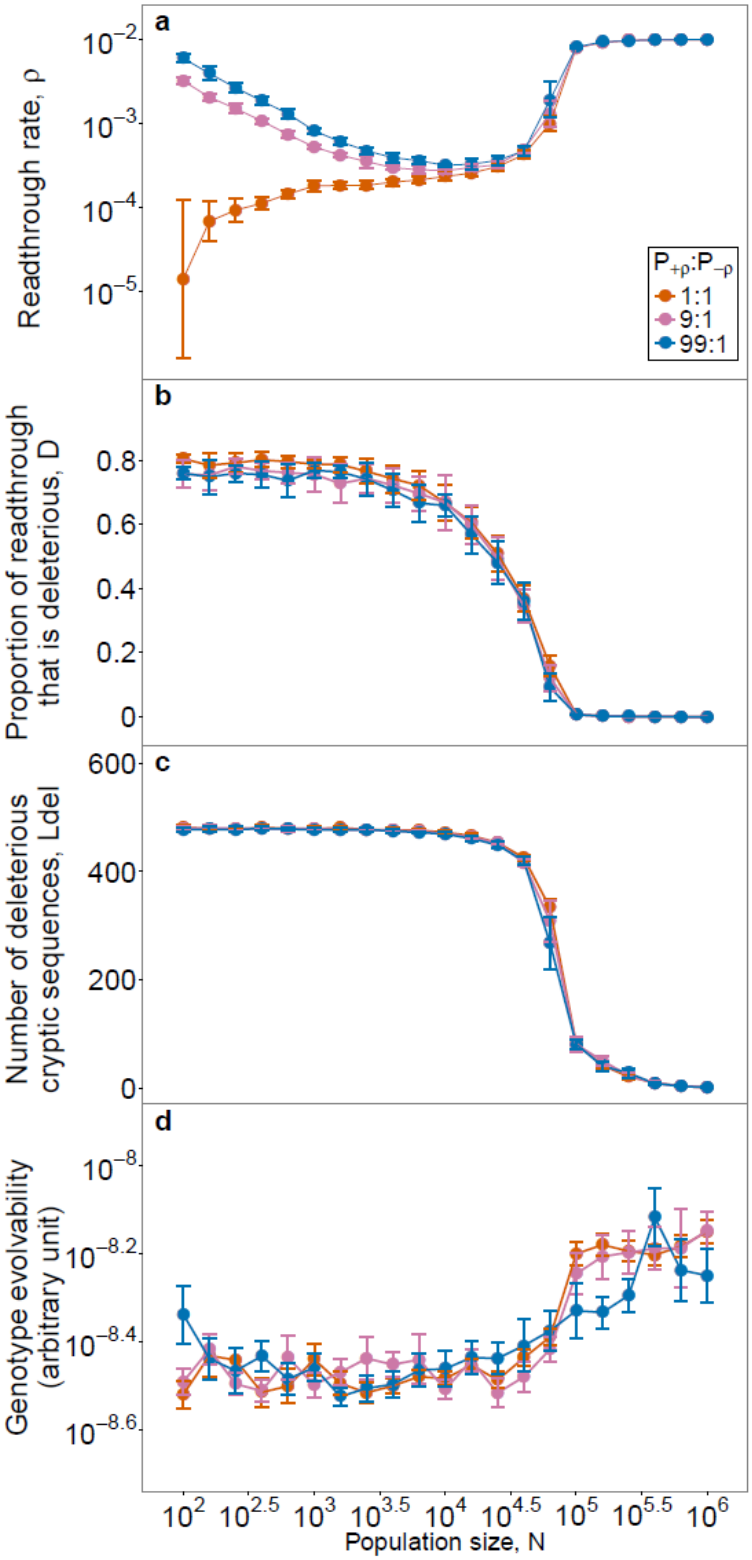

Figure 4: Mutation bias tends to increase ρ, such that even the global solution breaks down in sufficiently small populations. $P_{+\rho}$ is the probability that a mutation increases ρ, and $P_{-\rho}$ is the probability of a decrease. Each data point, (except those taken from Fig. 1 with $P_{+\rho}$:$P_{-\rho}$ = 1:1 and $N = 10^{3.6}$ to $N = 10^{6.0}$), is pooled from 5 replicates of high-ρ initial conditions and 5 replicates of low-ρ initial conditions. Because we assume multiplicative mutational effects to ρ, its value converges even for extremely small N. I.e., as ρ increases, the additive effect size $\Delta\rho$ of a typical mutation also increases, preventing it from passing through the drift barrier. For **a**, **b**, and **c**, data is shown as mean$\pm$SD. For **d**, data is shown as mean$\pm$SE. For **a** and **d**, these apply to log-transformed values. L = 600 and σ_E = 2.25.

Supplemental material for the manuscript

"Drift barriers to quality control when genes are expressed at different levels"

Xiong K, McEntee JP, Porfirio DJ, Masel J

Implementation of origin-fixation simulations

Origin-fixation models are often implemented via a crude rejection algorithm; large numbers of mutations are simulated, and each is accepted as a successful fixation event if and only if a random number sample from the uniform [0, 1] distribution falls below its (fairly low) fixation probability. For large *N*, this method is computationally slow when significant numbers of nearly neutral mutations must be sampled before one fixes with probability ~1/*N*. Given that our model posits only a relatively small range of possible mutations, we instead sampled only mutations that go on to become fixed, by sampling according to the relative values of "fixation flux", proportional to mutation rate × fixation probability for each of our six categories of mutation. In other words, we used a form of the Gillespie (1977) algorithm.

In a haploid population of size *N*, the probability of fixation of a new mutant into a resident population is given by

$$P_{fix} = \frac{1-e^{-s}}{1-e^{-Ns}} \quad (9)$$

where $s = w_{mutant}/w_{resident}-1$. It is then straightforward to calculate fixation flux values for all possible switches between benign and deleterious states:

$$f_{del\_to\_ben} = N\mu_{ben} \sum_{i \in loci\_with\_del\_crypt\_seq} P_{fix}(del\_to\_ben\_at\_i) \quad (10)$$

$$f_{ben\_to\_del} = N\mu_{del} \sum_{i \in loci\_with\_ben\_crypt\_seq} P_{fix}(ben\_to\_del\_at\_i) \quad (11)$$

Matters are slightly more complicated for quantitative mutations to α, β and ρ, because we must integrate the fixation flux over all possible sizes ($\Delta\alpha_k$, $\Delta\beta_k$, and $\Delta\log_{10}\rho$) for a mutation at a given locus, prior to summing across loci to arrive at the fixation flux for an entire mutational category:

$$f_\alpha = N\mu_\alpha \sum_k^K \int P_{fix}(\Delta\alpha_k)P(\Delta\alpha_k)d\Delta\alpha_k \quad (12)$$

$$f_\beta = N\mu_\beta \sum_k^K \int P_{fix}(\Delta\beta_k)P(\Delta\beta_k)d\Delta\beta_k \quad (13)$$

$$f_\rho = N\mu_\rho \int P_{fix}(\Delta\log_{10}\rho)P(\Delta\log_{10}\rho)d\Delta log_{10}\rho \quad (14)$$

where $P(\Delta\alpha_k)$, $P(\Delta\beta_k)$, and $P(\Delta\log_{10}\rho)$ are the probability densities for the magnitude of a given kind of mutation.

We use the quadrature method to calculate the integral over these possibilities, using a grid of 2000, limited for $\Delta\alpha_k$ to the interval $[-\alpha_k/\alpha-5\sigma_m/K, -\alpha_k/\alpha+5\sigma_m/K]$, for $\Delta\beta_k$ to the interval $[-\beta_k/\alpha-5\sigma_m/K, -\beta_k/\alpha+5\sigma_m/K]$, and for $\Delta\log_{10}\rho$, to the interval $[-10\sigma_\rho, \min(10\sigma_\rho , -\log_{10}\rho)]$. In the latter case, the number of grid intervals is reduced proportional to any truncation of the interval at $-\log_{10}\rho$.

For mutational co-options of benign cryptic sequences, the effect of replacing the value of α_k with that of $\alpha_k+\beta_k$ is fixed, but there is also a stochastic range of effects of initializing a new β_k and a new B_k (Eq. 15). Let $P(\beta_k')$ be the probability density of a new β_k given by Normal(0, $V(a, K, \sigma_m)$), and $P(B_k' = 1) = 1 - P(B_k' = 0)$ be the probability that a new B_k equals to 1, and hence the new β_k affects the trait value. The fixation flux associated with cooption mutations we obtained numerically by integration over the range [$-5\sigma_m/K$, $5\sigma_m/K$]:

$$f_{coopt} = N\mu_{coopt} \sum_{k \in loci\_with\_ben\_crypt\_seq}^{K} \left(\begin{array}{c} P(B_k' = 1) \int P_{fix}(\beta_k', B_k' = 1) P(\beta_k') d\beta_k' \\ + P(B_k' = 0) P_{fix}(B_k' = 0) \end{array} \right) \quad (15)$$

The expected waiting time before the current genotype is replaced by another is

$$\text{waiting time} = \frac{1}{\text{total fixation flux over all six categories}} \quad (16)$$

A standard Gillespie (1977) algorithm would calculate the realized waiting time as a random number drawn from an exponential distribution with this mean. Since we are only interested in the outcome of evolution, and not the variation in its timecourse, we used the expected waiting time instead, decreasing our computation time. The waiting time can be interpreted as the time it takes for a mutation destined for fixation to appear, neglecting the time taken during the process of fixation itself. Using this interpretation, we specify waiting times in terms of numbers of generations, based on our assumptions about absolute mutation rates.

We assign the identity of the next fixation event among the six categories according to probabilities proportional to their relative fixation fluxes, then we assign the identity within the category. For switches between benign and deleterious states, allocating a fixation event within a category according to the relative values of fixation fluxes is straightforward. For mutations to ρ, α, and β, and mutational co-option, we relax the granularity and cutoff assumptions of the grid-integration method when choosing a mutation within the category. Instead, we sample a mutational value of $\Delta\log_{10}\rho$ from Normal(ρ_{bias}, σ_ρ^2). We reject and resample $\Delta\log_{10}\rho$ if $\Delta\log_{10}\rho \geq -\log_{10}\rho$. Otherwise, we accept vs. reject-resample according to the fixation probability of that exact mutation, by comparing this probability to a random number uniformly distributed at [0, 1.1×the maximum fixation probability across the grid points previously calculated for $\Delta\log_{10}\rho$ during our grid calculation]. For $\Delta\alpha$ (or $\Delta\beta$), the procedure is conceptually similar but has a more complicated implementation. We first sample from Normal(0, $(\sigma_m/K)^2$). We then add the random number to each of the values of $-\alpha_k/a$, and calculate the sum of corresponding fixation probabilities across all loci k. We accept vs. reject-resample the mutation by comparing this sum to a random sample from a uniform distribution at [0, 1.1×the maximum corresponding fixation probability sum calculated during our grid calculation]. If the mutation is accepted, we allocate it to a locus k with probability proportional to their relative fixation probabilities. For mutational co-option of a benign cryptic sequence, the main effect is to replace α_k with $\alpha_k+\beta_k$, but there are also subtler effects arising from the reinitialization of the new cryptic sequence. Any of the k loci for which $B = 1$ are eligible for co-option, the new value of B may be either 0 to 1, and the new β_k may take a range of values. Each combination of k and new B has its own fitness flux, and the first choice is among these {k, B} pairs. Next we sample

β_k from Normal(0, $(\sigma_m/K)^2$); for a new B equal to 0 we always accept the result, and for new B equal to 1, we accept vs. reject-resample β_k by comparing its probability of fixation to a random sample from a uniform distribution at [0, 1.1×the maximum corresponding fixation probability sum calculated during our grid calculation].

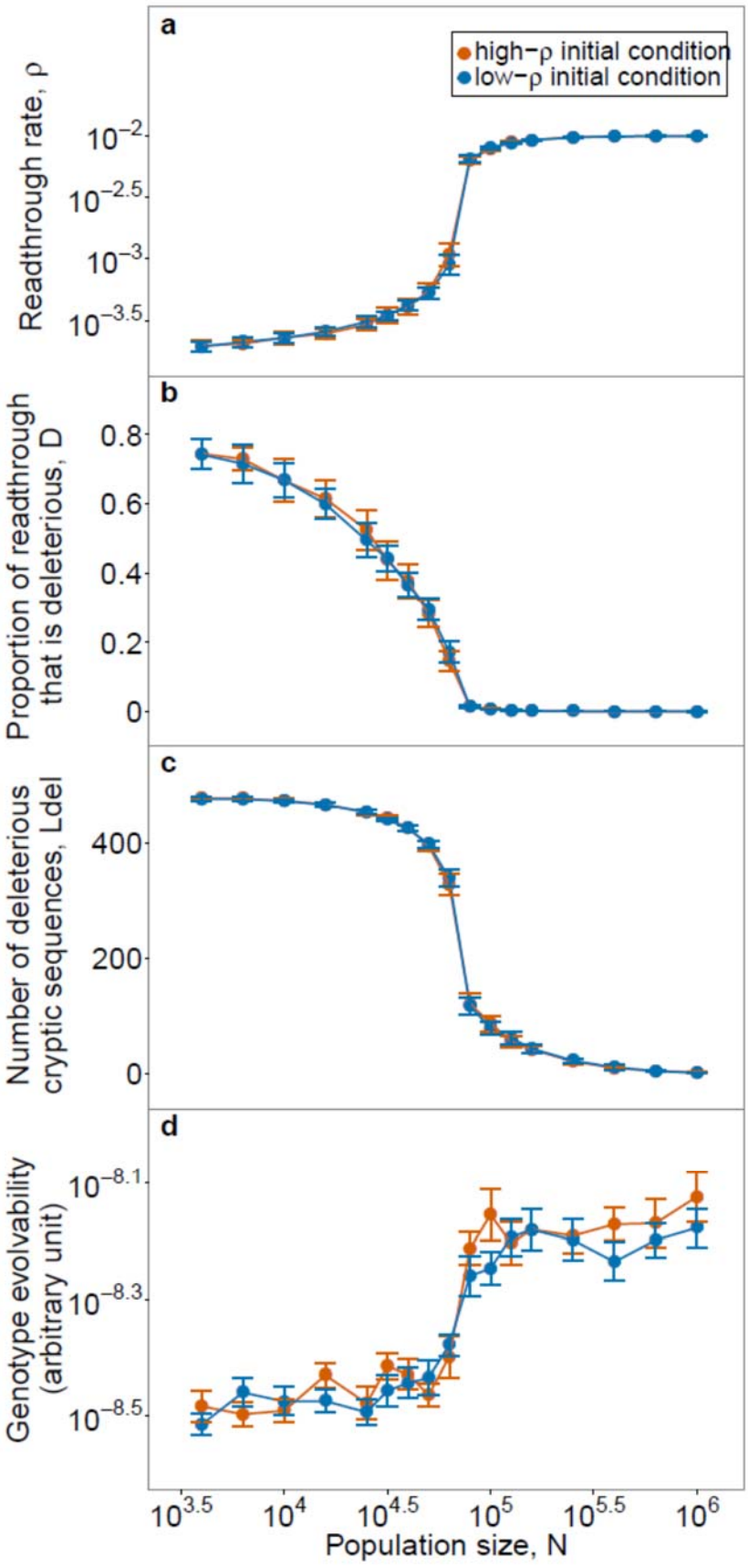

Figure S1: At σ_E = 2.25, the final state of the evolutionary simulation does not depend on the initial conditions. The data shown here is the same as that shown pooled in Fig. 1.

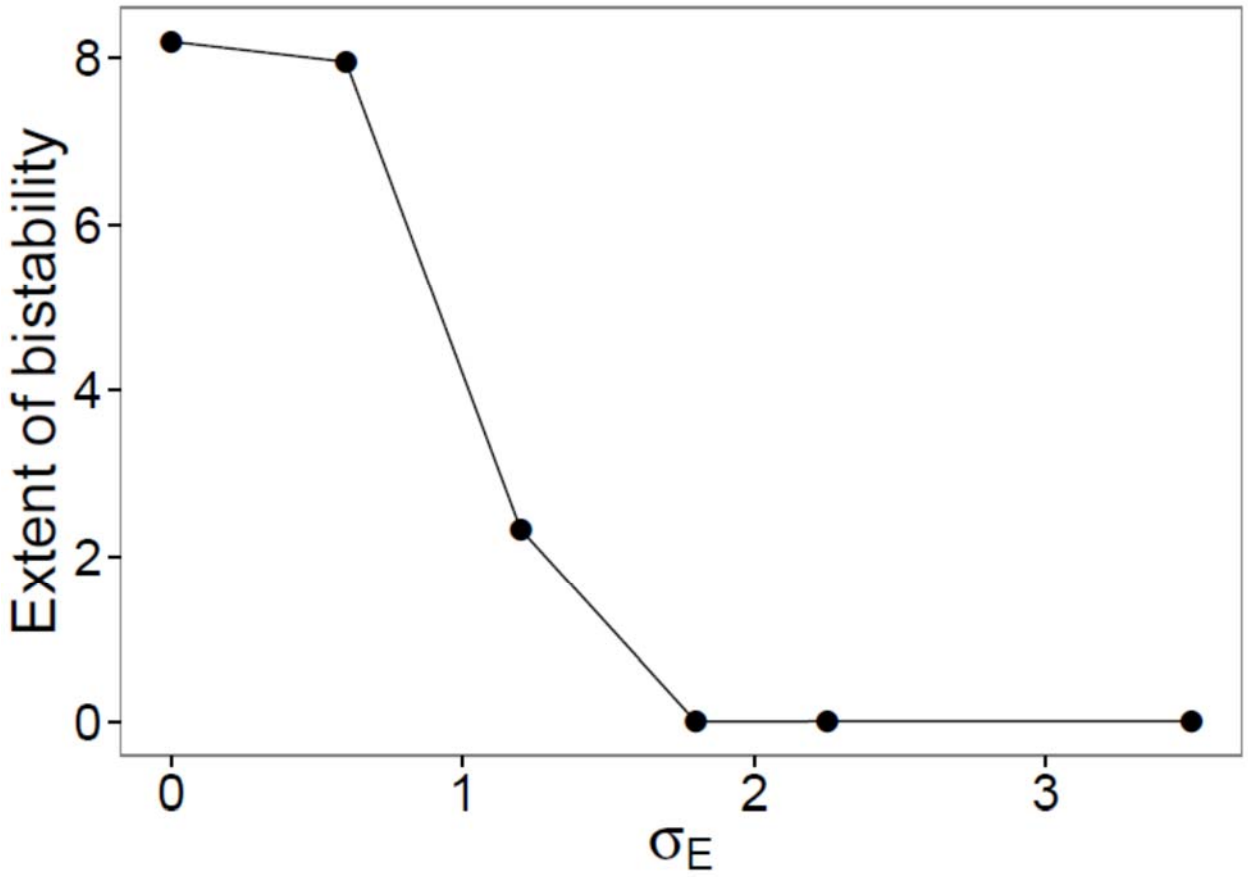

Figure S2: The range of population sizes that exhibit significant bistability drops dramatically even for σ_E < 2.25. We used average values of ρ towards the end of the simulations as a measure of the solution found by each replicate. For each initial condition, we averaged over five replicates (except for σ_E = 0, 2.25, and 3.5, where we reused the 20 replicates of Fig. 1), and over each of the values of N between $10^{3.6}$ to 10^{6}, with an increment of $10^{0.2}$. The extent of bistability was assessed as $\sum_N(\log_{10}\bar{\rho}_{init\_low} - \log_{10}\bar{\rho}_{init\_high})^2$. L = 600.

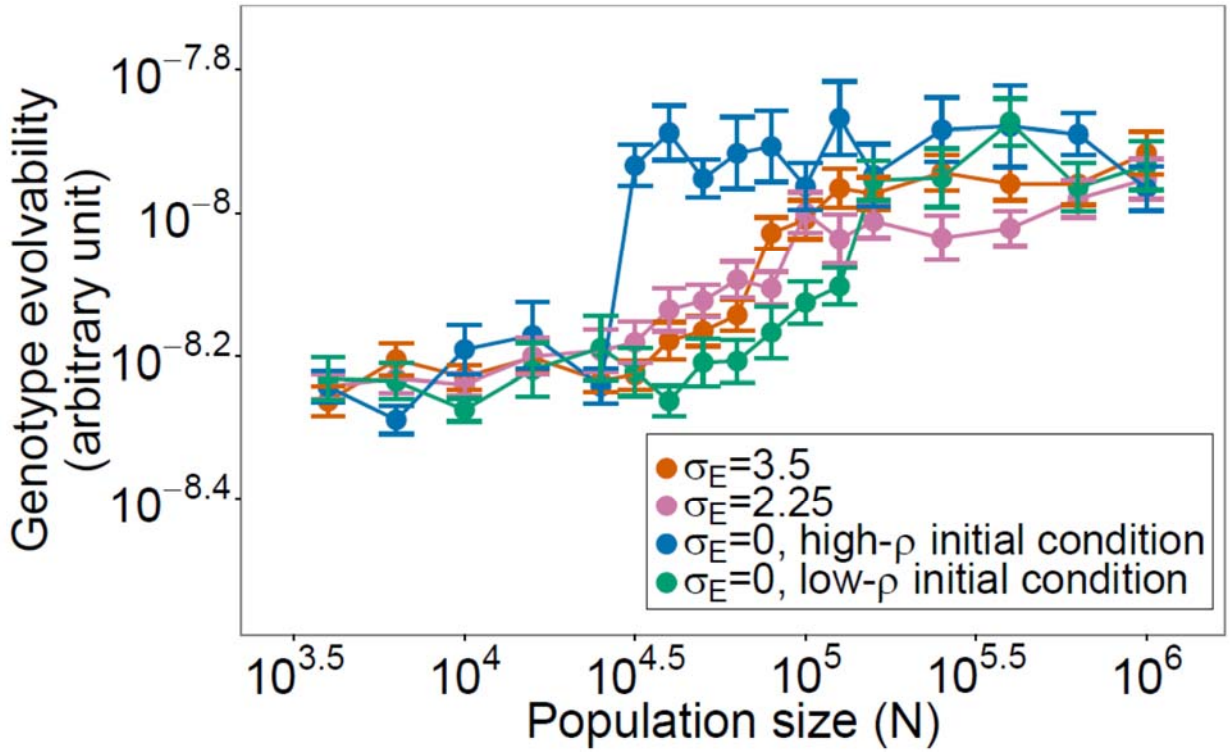

Figure S3: The time taken for the trait to approach the new value of x_{opt} behaves similarly to the recovery time of fitness shown in Fig. 1**d**. The same simulations were used as in Fig. 1. At σ_E = 2.25 and σ_E = 3.5, we pooled the results from high-ρ and low-ρ conditions. Evolvability is shown as mean$\pm$SE of the log-transformed values. L = 600.

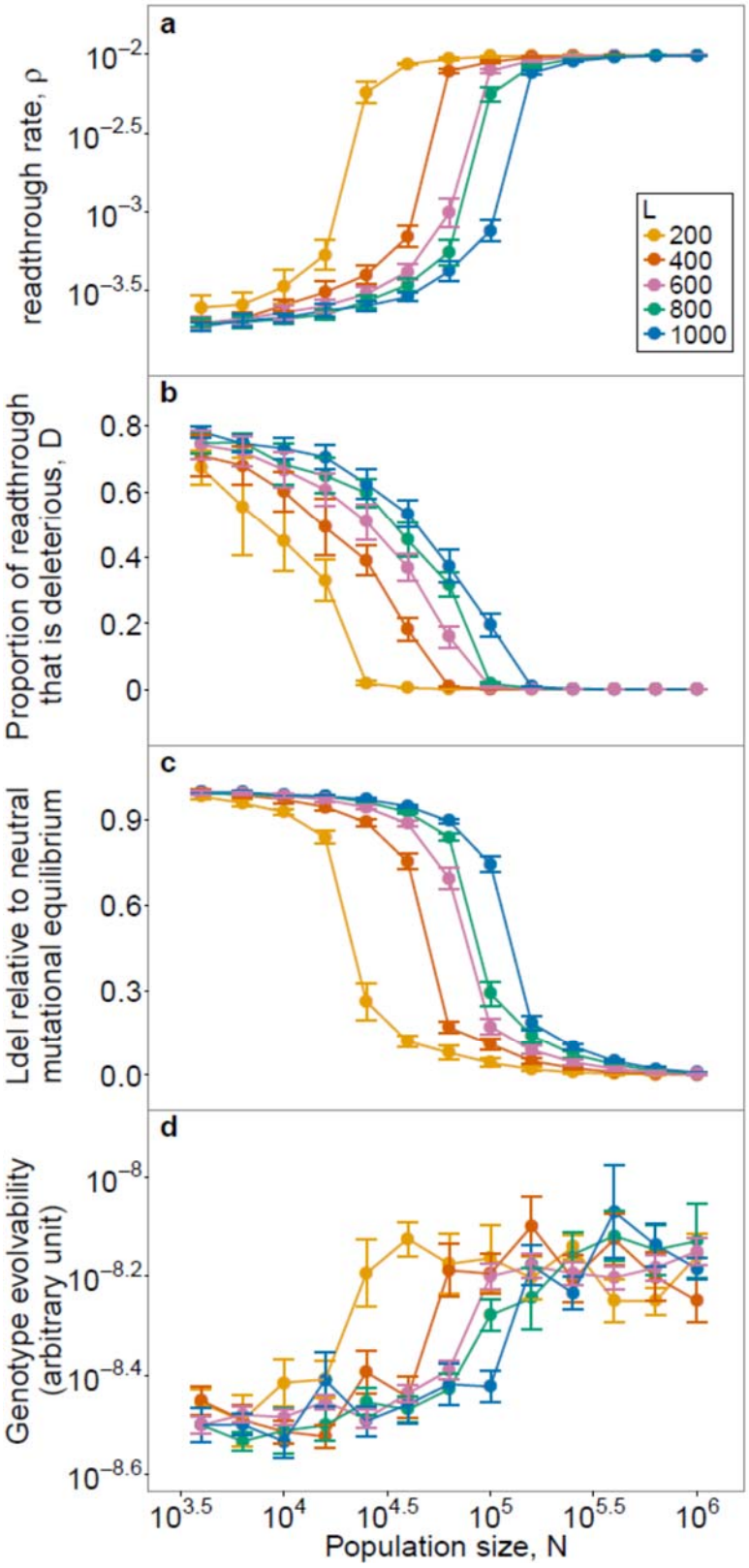

Figure S4: Changing the number of loci does not qualitatively change our results. Quantitatively, fewer loci favor more local solutions. Changing *L* alters the average contribution of each locus to *D.* This alters the average strength of selection on each locus, independent of population size. Therefore, the same solutions, characterized by the values of *ρ* and *D*, are "shifted" to small values of *N* as *L* decreases. While *L* changed, we held the number of quantitative trait loci constant at 50. For *L* = 600, we reused the results shown in Fig. 1. For other values of *L*, five replicates were run for each of the two initial conditions. We pooled results from both initial conditions across all values of *L*. We normalized L_{del} to the neutral mutational equilibrium of $L \times \mu_{del}/(\mu_{del}+\mu_{ben})$. For panels **a** to **c**, data is shown as mean$\pm$SD. For **d**, data is shown as mean$\pm$SE. For **a** and **d**, these apply to log-transformed values. $\sigma_E = 2.25$.

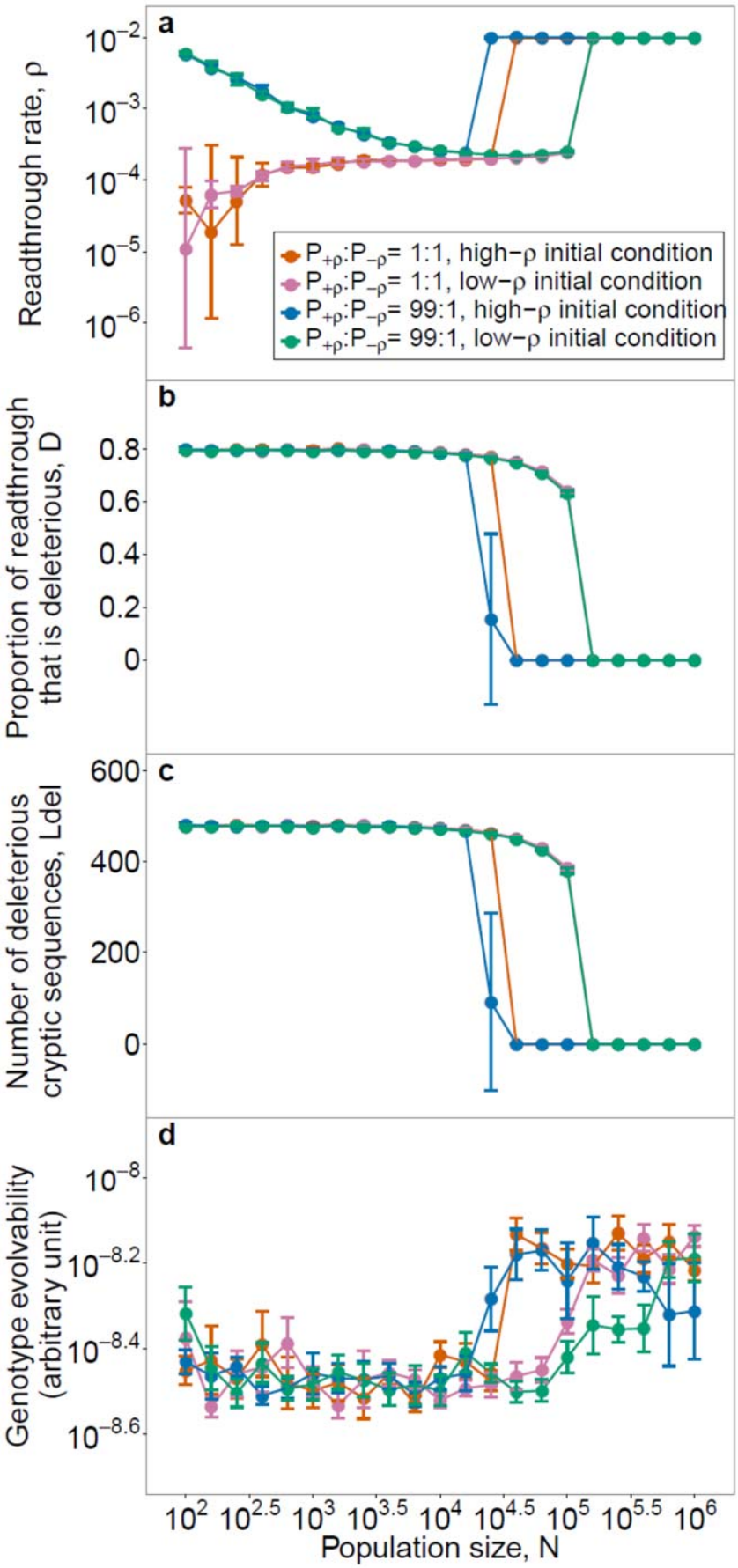

Figure S5: Fig. 4 results (that the global solution breaks down in sufficiently small populations) remain true in the absence of variation of expression levels. Data points between $N = 10^{3.6}$ to $N = 10^{6.0}$ and $P_{+\rho}:P_{-\rho} = 1:1$, are reused from Fig. 1; for the others, we performed 5 replicates for each condition. For panels **a** to **c**, data is shown as mean±SD. For **d**, data is shown as mean±SE. For **a** and **d**, these apply to log-transformed values. $L = 600$.

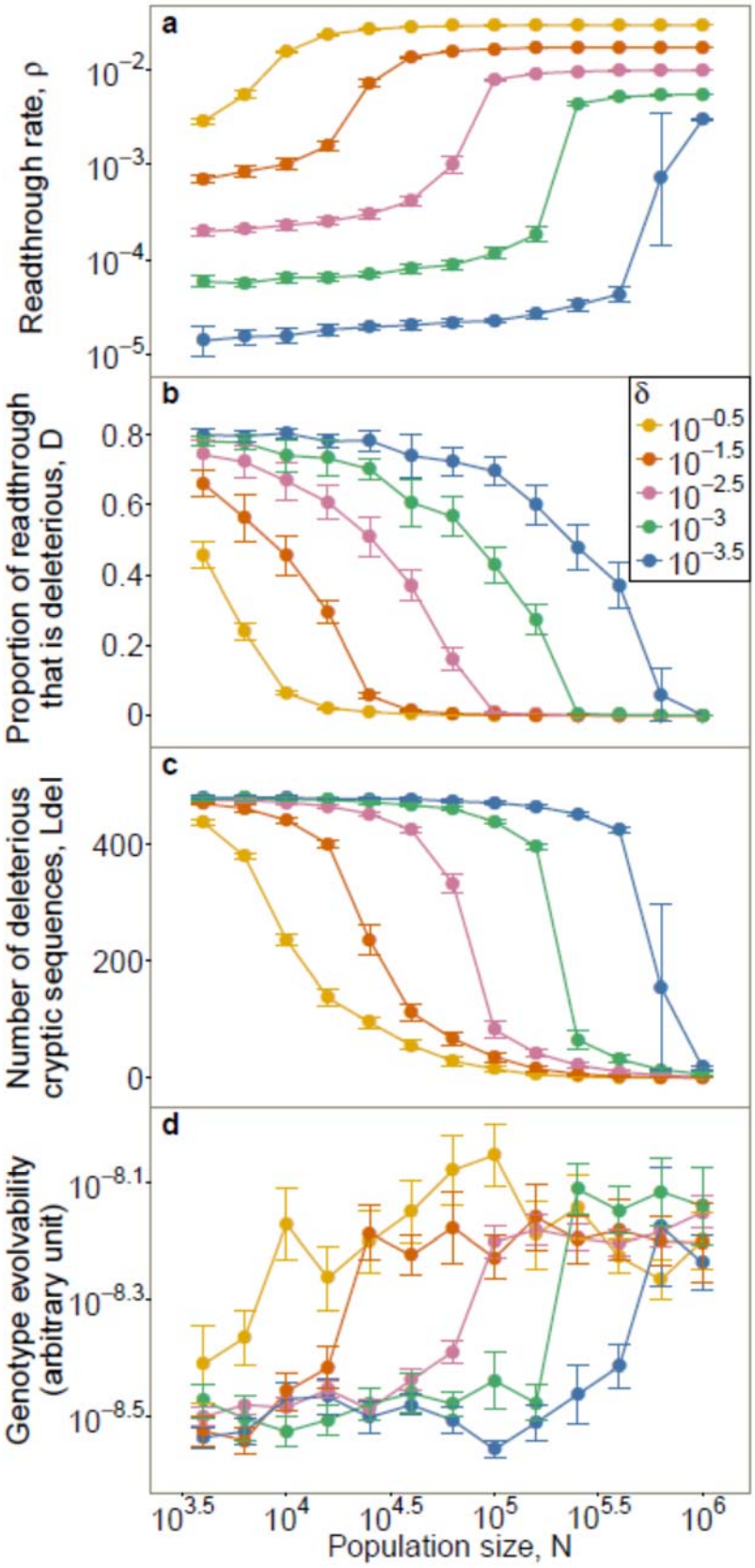

Figure S6: Increasing the cost of quality control δ expands global solutions to smaller populations and reduces the differences in error rates as a function of population size. For $\delta = 10^{-2.5}$, we reused the data from Fig. 1; for each of the other values of δ, we ran 5 replicates from the high-ρ initial condition and 5 from the low-ρ initial condition. Each data point represents the pooled results from the two initial conditions. For panels **a** to **c**, data is shown as mean$\pm$SD. For **d**, data is based on time to fitness recovery and is shown as mean$\pm$SE. For **a** and **d**, the mean, SD and SE are calculated on log-transformed values. The large error bars at $N = 10^{5.8}$ under $\delta = 10^{-3.5}$ across all panels are due to different initial conditions, which is a sign of bistability. $L = 600$, $\sigma_E = 2.25$.

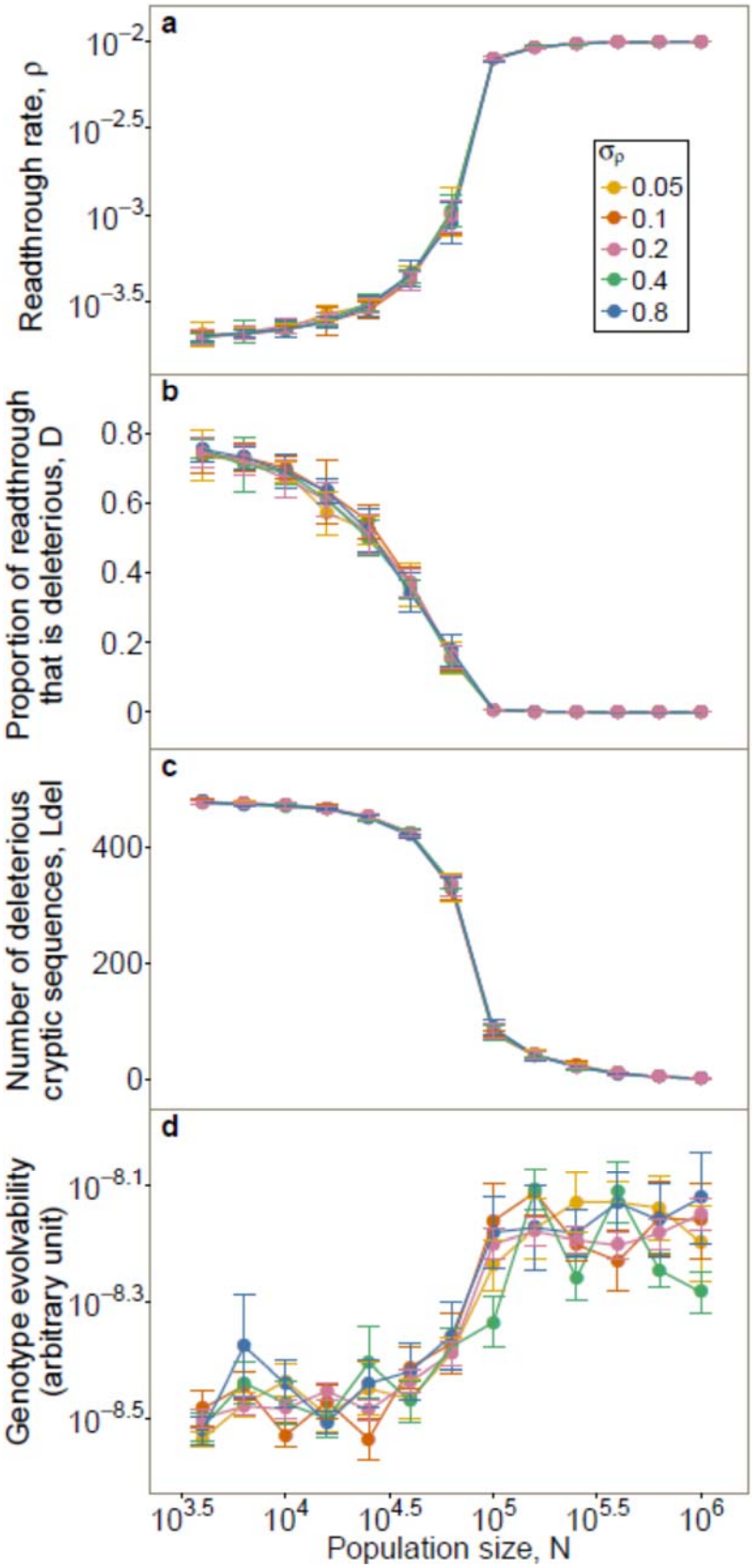

Figure S7: The variance in the magnitude of mutations to ρ does not affect a population's solution to error or evolvability. For $\sigma_\rho = 0.2$, we reused the data from Fig. 1; for each of the other values of σ_ρ, we ran 5 replicates from each of the two initial conditions. We pooled results from the two initial conditions for each data point. For panels **a** to **c**, data is shown as mean$\pm$SD. For **d**, data is based on time to fitness recovery and is shown as mean$\pm$SE. For **a** and **d**, these apply to log-transformed values. $L = 600$, $\sigma_E = 2.25$.

Table S1: Summary of model parameters

Group	Parameter	Biological meaning	Exploration	Parameter values in model[1]	Influence on global v. local solutions
Selection for local vs. global solution	σ_E^2	Variance of $\log_2$ expression among loci	Fig. 1, Fig. S2	5.1 (0-12.3)	Central finding: lower σ_E^2 promotes dichotomy
	c	Cost of misfolding	Fig. S3[2]	20 (7-28[2])	Large c makes ρ smaller, with a slightly larger impact on global solutions, and expands the bistable region to smaller populations.
	δ	Scaling of quality control costs	Fig. S6	$10^{-2.5}$ ($10^{-0.5}$-$10^{-3.5}$)	Higher cost makes ρ larger, with a larger impact on global solutions, and expands global solutions to smaller populations
	L	Total number of loci	Fig. S4, Fig. S2[2]	600 (200-1000)	Lower L shift the transition between local and global solutions to smaller populations, but maintain the shape of the transition
Mutation bias for local vs. global solution	μ_{del}	Rate of benign-to-deleterious mutations	Fig. 3	μ_{del}:μ_{ben} = 4:1 (1:1-99:1)	Stronger mutation bias lowers ρ and shifts the transition between local and global solutions to larger populations
	μ_{ben}	Rate of deleterious-to-benign mutations			
	$P_{+\rho}\times\mu_\rho$	Rate of mutations that increase ρ	Fig. 4, Fig. S5	$P_{+\rho}$:$P_{-\rho}$ = 1:1 (1:1-99:1)	Mutation bias prevents extremely small populations from reducing ρ
	$P_{-\rho}\times\mu_\rho$	Rate of mutations that decrease ρ			
	σ_ρ^2	var(mutations to ρ)	Fig. S7	0.04 (2.5×10^{-3}-0.64)	No apparent influence
Relevant only for quantitative effects and evolvability (of peripheral interest to our central findings)	K	Number of quantitative trait loci	Fig. S7[2]	50 (5-50[2])	-
	a	Speed that α and β revert to mean	Fig. S10[2]	750 (250-2000[2])	
	μ_{coopt}	Rate of co-option mutations	-	2.56×10^{-9}	
	μ_α	Rate of mutations to α	-	3×10^{-7}	
	μ_β	Rate of mutations to β	-	3×10^{-8}	
	σ_m^2	σ_m^2/K = var(mutations to α and β)	Fig. S8[2]	0.25 (0.04-1[2])	
	σ_f	Strength of selection on trait	No loss of generality when σ_m^2 only is explored	0.2	

[1] The numbers outside parentheses are the default values and the numbers inside indicate the parameter range explored.
[2] Rajon and Masel (2011)

Supplementary References:

Rajon, E., and J. Masel, 2011 The evolution of molecular error rates and the consequences for evolvability. Proc. Natl. Acad. Sci. U.S.A. 108**:** 1082-1087.